

## Improvements in the GFDL Hurricane Prediction System

YOSHIO KURIHARA, MORRIS A. BENDER, ROBERT E. TULEYA, AND REBECCA J. ROSS\*

*Geophysical Fluid Dynamics Laboratory/NOAA, Princeton, New Jersey*

(Manuscript received 24 May 1994, in final form 10 January 1995)

### ABSTRACT

The hurricane model initialization scheme developed at GFDL was modified to improve the representation of the environmental fields in the initial condition. The filter domain defining the extent of the tropical cyclone in the global analysis is determined from the distribution of the low-level disturbance winds. The shape of the domain is generally not circular in order to minimize the removal of important nonhurricane features near the storm region. An optimum interpolation technique is used to determine the environmental fields within the filter domain. Outside of the domain, the environmental fields are identical to the original global analysis. The generation process of the realistic and model-compatible vortex has also undergone some minor modifications so that reasonable vortices are produced for various data conditions. The upgraded hurricane prediction system was tested for a number of cases and compared against the previous version and yielded an overall improvement in the forecasts of storm track. The system was run in an automated semioperational mode during the 1993 hurricane season for 36 cases in the Atlantic and 36 cases in the eastern Pacific basin. It demonstrated satisfactory skill in the storm track forecasts in many cases, including the abrupt recurvature of Hurricane Emily in the Atlantic and the landfall of Hurricane Lidia onto the Pacific coast of Mexico.

### 1. Introduction

The purpose of this paper is to describe changes made to the initialization scheme, which was developed at the Geophysical Fluid Dynamics Laboratory (GFDL) [Kurihara et al. (1993a); hereafter referred to as KBR] for the multiply nested movable mesh (MMM) hurricane model, and to present results of the storm track forecasts using the modified prediction system.

It has been suggested that accurate representation of both the large-scale flow and the inner structure of the tropical cyclone in initial conditions of hurricane models can significantly contribute to improvements in dynamical prediction of hurricanes (e.g., Anthes 1982). A recent numerical study using a hurricane model with much increased horizontal resolution (Bender et al. 1993) demonstrated that improved initial conditions could not only increase the accuracy in the storm track forecasts but also yield skill in the prediction of the intensity and wind distribution.

For the large-scale flow, hurricane models usually rely on an operational global analysis such as the one from the National Meteorological Center (NMC). As

the resolution of the global model increases, tropical cyclones have become more clearly identifiable in the global analyses. However, the resolution of the T126 spectral model in use at NMC is still by far too coarse to accurately resolve the structure of the storm's interior. For instance, the minimum surface pressure 1010 hPa of Hurricane Emily in the global analysis at 0000 UTC 30 August 1993 was much weaker than the observed value 976 hPa, and the maximum storm wind at 850 hPa barely exceeded  $17 \text{ m s}^{-1}$ . Under these circumstances, the KBR scheme was formulated to provide an operationally feasible means to prepare initial conditions for hurricane models having much higher resolution than the global model. Without initialization, the initial structure of the storm is inaccurate, and the storm motion can be erratic at the start of the model integration as the analyzed vortex adjusts to much finer model resolution. The KBR scheme is designed to replace the vortex in the global analysis with a specified vortex that is more realistic and compatible with the hurricane model. A crucial aspect of the scheme to the correct prediction of the hurricane movement is a reasonable determination of the environmental field from the global analysis because the hurricane vortex will be approximately advected by the environmental wind in which it is embedded.

The GFDL hurricane prediction system involving the KBR initialization scheme was applied in the 1992 hurricane season in near-real-time mode to 20 cases. Considerable skill was shown for the hurricane track forecasts especially in cases of strong storms. The sys-

\* Current affiliation: Air Resources Laboratory/NOAA, Silver Spring, Maryland.

Corresponding author address: Dr. Yoshio Kurihara, NOAA/GFDL, Princeton University, Post Office Box 308, Princeton, NJ 08542.

tem accurately predicted the landfall of Hurricane Andrew onto the Louisiana coast two days in advance (Kurihara et al. 1993b) and the recurvature of Hurricane Iniki in the Pacific. However, predictions were sometimes less accurate in cases of weak storms.

Following the 1992 season, the performance and capability of the GFDL prediction system were extensively analyzed and evaluated. Inaccuracies in the prediction of some weak storms were determined to be related to the representation of the environmental flow field in the storm area. In particular, the automated procedures for removal of the analyzed vortex from the global analysis tended also to remove features in the storm vicinity that on visual inspection would not be considered hurricane-related features. These environmental features sometimes played a significant role in the storm movement. In the present study, the extent of the analyzed vortex is more restrictively defined. This, combined with an application of the optimum interpolation technique for determining the environmental field in the storm area, enables the nonhurricane features to be retained in the initial conditions of the model. The new method was tested for 23 cases and yielded a reduction in the average track forecast error compared with the original KBR scheme. The revised initialization scheme will be described in section 2.

The upgraded GFDL hurricane prediction system was run in semioperational mode during the 1993 hurricane season on 36 Atlantic cases and 36 eastern Pacific cases. The forecast results are presented in section 3, and the summary and remarks on the prediction system are given in section 4.

## 2. Improvements in the initialization technique

### a. Basic framework and issues

The basic strategy of the hurricane model initialization used in the present study is the same as that developed by KBR. Schematically, the scheme to construct a realistic initial field can be expressed as

$$\begin{aligned} (\text{initial field}) &= (\text{global analysis}) \\ &\quad - (\text{analyzed vortex}) + (\text{specified vortex}). \end{aligned}$$

The initialization begins with the removal of the hurricane vortex in the global analysis. As in KBR, this process is also expressed as the determination of the environmental field where

$$\begin{aligned} (\text{environmental field}) &= (\text{global analysis}) \\ &\quad - (\text{analyzed vortex}). \end{aligned}$$

In the following, the KBR method to determine the environmental field is briefly described while establishing the terminology to be used for later discussion. The global analysis field is first partitioned into a large-scale component, called the basic field, and the deviation from it, called the disturbance field; that is,

$$\begin{aligned} (\text{global analysis}) &= (\text{basic field}) \\ &\quad + (\text{disturbance field}). \end{aligned}$$

The disturbance field includes the smaller-scale variability depicting the analyzed vortex as well as any other nonbasic features. The next step is to separate the analyzed storm, called the hurricane component, from the disturbance field. The remainder is called the nonhurricane component for convenience; namely,

$$\begin{aligned} (\text{disturbance field}) &= (\text{hurricane component}) \\ &\quad + (\text{nonhurricane component}). \end{aligned}$$

In the KBR approach, it is assumed that the hurricane component is confined within an appropriately determined domain, called the filter domain. Accordingly, the disturbance field outside of the filter domain is defined to be entirely the nonhurricane component. Within the filter domain, the disturbance field is primarily due to the hurricane component. As the distance from the storm center increases, however, the storm's signal weakens, and a greater part of the disturbance field may be due to the nonhurricane component. In the GFDL initialization scheme, the nonhurricane component within the filter domain is determined from the disturbance field at the filter domain boundary. Thus, the analyzed vortex, which is represented by the hurricane component, is implicitly defined as the deviation of the disturbance field from the nonhurricane component. The environmental field is then obtained by combining the nonhurricane component with the basic field; that is,

$$\begin{aligned} (\text{environmental field}) &= (\text{basic field}) \\ &\quad + (\text{nonhurricane component}). \end{aligned}$$

It is clear that the environmental field is identical to the global analysis outside the filter domain. Within the filter domain, the hurricane component of the disturbance field is effectively removed from the global analysis through the use of the environmental field. The initialization is completed with the addition of a realistic storm vortex, which is generated and specified as a new hurricane component, onto the environmental field.

The major issue addressed in this section is the improved determination of the environmental field. A guideline previously set in KBR for this process is that the environmental field should smoothly vary across the filter domain. As suggested in section 1, the environmental field also should retain important nonhurricane features near the storm. The two improvements presented here are designed to more accurately represent the nonhurricane component near the storm. The first improvement is in the determination of the filter domain defining the extent of the analyzed vortex in the disturbance field, while the other involves a change of the method to construct the nonhurricane component

within the filter domain. Another subject treated in this section is the scheme to generate the specified vortex. Some small changes are introduced in the computational procedures in the scheme so that the scheme produces more reasonable vortices in a variety of input data conditions. No changes were made in the merging procedure of the generated vortex with the environmental field and in the final static initialization step of the KBR scheme.

*b. Splitting of the global analysis field*

In this and subsequent two subsections, the low-level wind field ( $\sigma = 0.85$ ,  $\sigma$  being the pressure normalized by the surface value) for a case of Hurricane Florence (1988) is used to illustrate the modified initialization procedures. Lord (1993, personal communication) suggested this case would be particularly suitable to demonstrate the advantages of the new technique because of the presence of a well-defined circulation center to the northeast of the hurricane (Fig. 1a).

The first step of the initialization is to split the global analysis field into the basic and disturbance fields. The basic field represents the large-scale general features of the analysis, and the disturbance field the deviation from it. For example, the low-level winds in the global analysis (Fig. 1a) is split into the two fields (Fig. 1b and Fig. 1c). This was achieved with repeated use of a local filtering operator (KBR) that does not cause sharp-scale cutoff in the separated fields.

*c. Determination of the filter domain*

As in KBR, the goal in the determination of the filter domain is to define a region that completely contains the analyzed vortex. Visually, such a region is detectable as an area centered on the storm position with strong gradients in the field of the tangential component of the disturbance wind. For example, Fig. 2a shows this field for the case of Florence. The challenge with Florence is to define a filter domain that retains the circulation to the northeast of the storm (Fig. 2b, same as Fig. 1c) as part of the nonhurricane component. It seems this circulation had an important influence on the storm track forecast. Whether this circulation is retained outside of the filter domain or not depends on the definition of the extent of the filter domain.

For strong tropical cyclones in a relatively quiescent environment, the KBR assumption of a circular filter domain is valid. However, the weaker gradients in a less intense tropical cyclone, especially when combined with a nonhurricane feature as in Florence, can result in a less symmetric tangential wind field. In the previous scheme, the filter domain was determined from the profile of the circular mean of the disturbance wind speed. This occasionally resulted in an erroneously large circular filter domain that tended to include the nonhurricane feature. In the new technique, the ex-

tent of the filter domain is determined from the disturbance winds at  $\sigma = 0.85$  (Fig. 2b) by examining the profile of their tangential component (Fig. 2a) along each of 24 radial directions ( $15^\circ$  angle separation with respect to the appropriately defined storm center). The filter domain thus defined may take a polygonal shape (Fig. 2, thick solid lines) and is intended to keep the nonhurricane circulations outside of the filter domain. Note that for strong storms the filter domain determined in this manner is usually still approximately circular. An advantage of using the tangential wind rather than the wind speed is that since it is computed relative to the tropical cyclone, it can differentiate the storm circulation more clearly from the adjacent systems. A problem of using the tangential wind is its dependency on the accuracy in the defined center position. This property, however, is conversely utilized in the present method to reasonably define the center position. A new formula to identify the center position of the storm in the disturbance wind field is presented below followed by a description of the modified scheme to determine the filter domain.

A more accurate positioning of the storm center than that of KBR is achieved by calculating a first-guess position from the distribution of the low-level disturbance wind speed and adjusting it to the most likely center position. The first-guess calculation is based on a simple idea that the wind speed is large in the storm region. Specifically, the first-guess position ( $\lambda_0^*$ ,  $\varphi_0^*$ ) is set to the location of the centroid of the disturbance wind speed  $V_{Dij}$  within a  $11^\circ \times 11^\circ$  subdomain centered at the grid point nearest to the observed storm position:

$$\lambda_0^* = \frac{\sum w_{ij} V_{Dij} \lambda_{ij} \Delta S_{ij}}{\sum w_{ij} V_{Dij} \Delta S_{ij}}, \quad \varphi_0^* = \frac{\sum w_{ij} V_{Dij} \varphi_{ij} \Delta S_{ij}}{\sum w_{ij} V_{Dij} \Delta S_{ij}},$$

where  $i$  and  $j$  are the gridpoint indices,  $\Delta S_{ij}$  is the area assigned to the grid point. The weight factor  $w_{ij}$ , which controls the influence of a particular grid point, is a function of each grid point's distance  $r$  from the subdomain center:

$$w_{ij} = \begin{cases} 1, & r \leq d \\ \exp\left[-\left(\frac{r-d}{D}\right)^2\right], & r > d; \end{cases}$$

$$d = 200 \text{ km}, \quad D = 400 \text{ km}.$$

Although the weight factor is small at large radii, the disturbance winds near the subdomain boundary can still affect the above positioning. The idea used in the adjustment of the first-guess position is that, given a hurricane-like vortex, a peak appearing in the profile of the azimuthal mean of the tangential component of flow (computed relative to the coordinate origin) will be highest when the coordinate origin is closest to the vortex center. Accordingly, for each grid point within a  $7^\circ \times 7^\circ$  area centered at the grid point nearest the first-guess

## HURRICANE FLORENCE (0000 UTC 9 SEPTEMBER 1988)

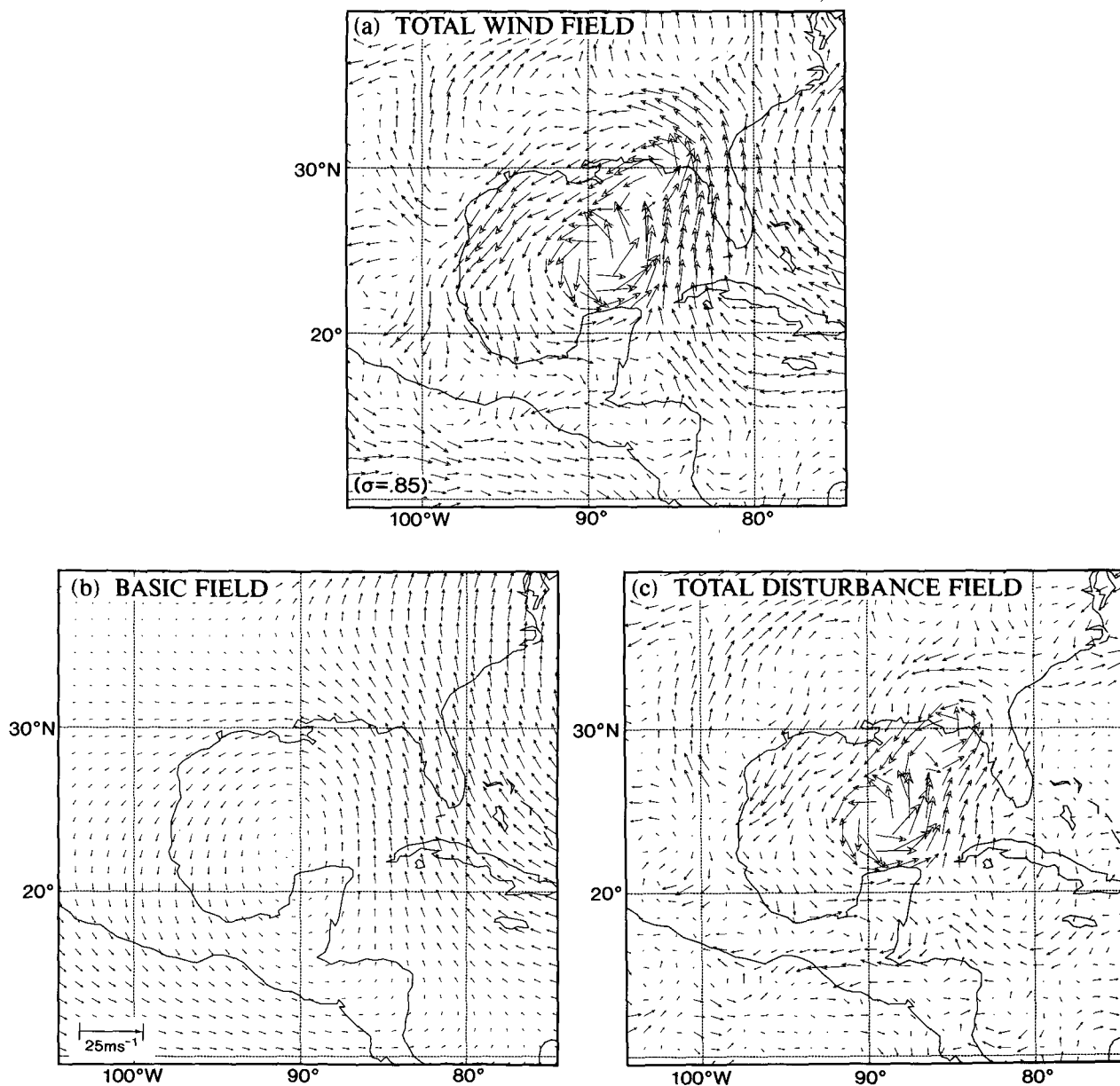


FIG. 1. (a) The total low-level ( $\sigma = 0.85$ ) wind field of Hurricane Florence at 0000 UTC 9 September 1988. The field (a) is split into (b) the basic field and (c) total disturbance field. Scale of wind vector arrows shown in (b) applies to all panels.

position  $(\lambda_0^*, \varphi_0^*)$ , the azimuthally averaged tangential component of the disturbance wind is computed at  $0.2^\circ$  radial intervals out to a distance of  $6^\circ$ , and the maximum value of each profile is determined. To compute an azimuthal average for a given radius, winds at latitude-longitude grid points are bilinearly interpolated to 24 points on the circle. The grid point associated with the profile containing the largest maximum value is consid-

ered as the most likely center of the analyzed vortex (shown by the hurricane symbol in Fig. 2a).

The extent of the filter domain is determined by testing the radial profiles of  $v_{\tan}(r, \theta)$ , the tangential component of the disturbance wind, in each of the 24 directions originating from the vortex center defined above. Specifically each profile is tested outward at an increment of  $0.1^\circ$  interval from an appropriate starting

### HURRICANE FLORENCE (0000 UTC 9 SEPTEMBER 1988)

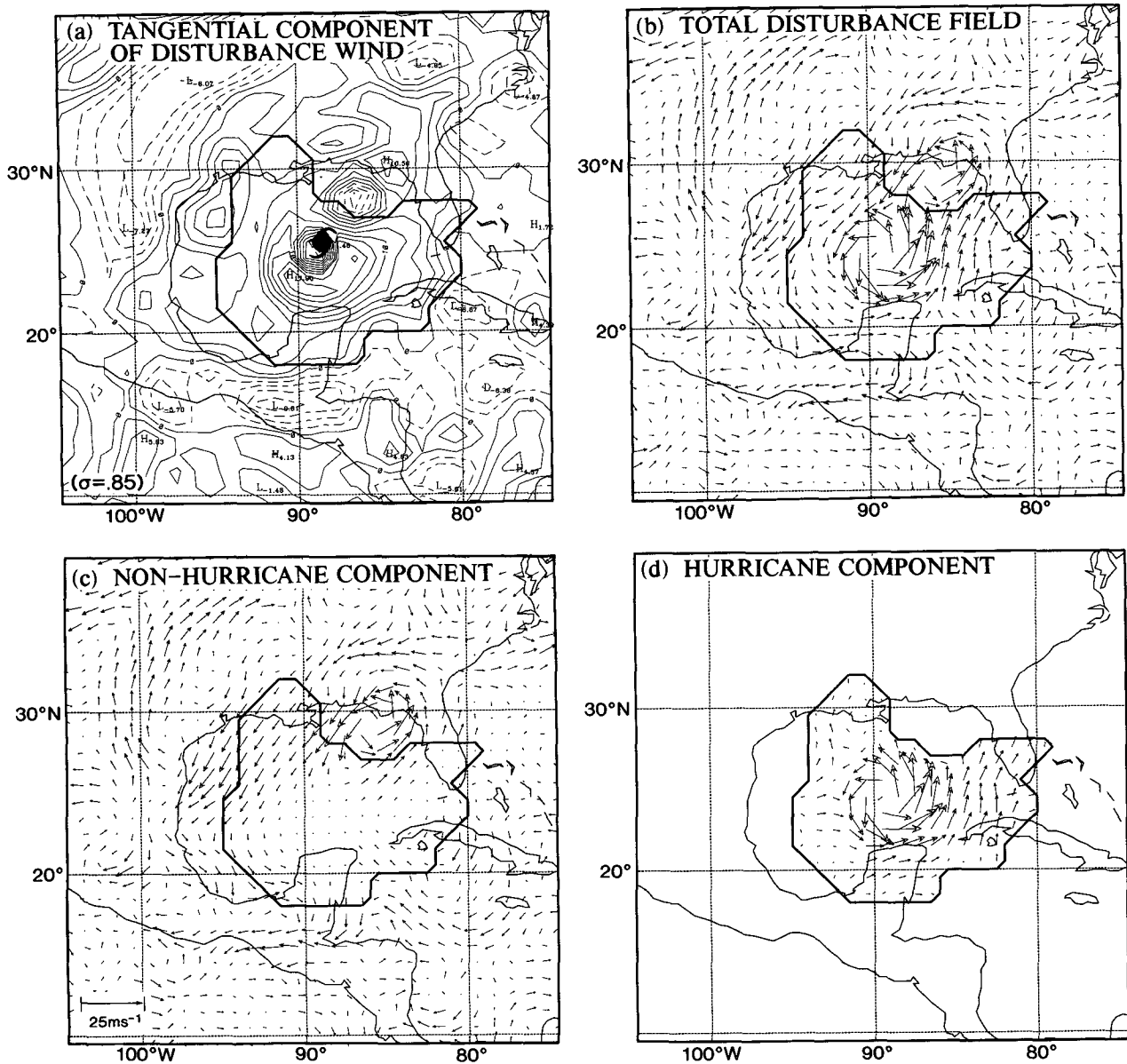


FIG. 2. (a) The tangential component of the disturbance wind with respect to the vortex center ( $2 \text{ m s}^{-1}$  contour interval; dashed lines for negative values) and the filter domain determined by the new scheme (bounded by a thick solid line). The center of analyzed vortex is shown by the hurricane symbol. The difference between the total disturbance field (b) (same as Fig. 1c, except for indicating the filter domain) and the nonhurricane component (c) is the hurricane component (d).

radius (see appendix A) to determine the radius called  $r_f(\theta)$ . This radius is defined as the radius of the point where the condition  $\nu_{\text{tan}} < 6 \text{ m s}^{-1}$  and  $-\partial\nu_{\text{tan}}/\partial r < 4 \times 10^{-6} \text{ s}^{-1}$  is met for the second time as the testing proceeds outward or the condition  $\nu_{\text{tan}} < 3 \text{ m s}^{-1}$  is met. As a practical constraint, the radius is bounded by 1200 km. Note that to define the domain of the storm, certain criteria that depend on the characteristics of the analyzed storm are required. The above empirical con-

ditions, which were the same as those applied in KBR to the azimuthal mean wind speed, were found to be appropriate for determining storm domains in various cases appearing in the present NMC global analysis. The test essentially seeks the edge of the region of steep gradient in the tangential wind component (e.g., Fig. 2a). Since  $\nu_{\text{tan}}$  typically decreases with increasing radius, the first criterion is likely to find the point, if any, where the initially steep gradient in  $\nu_{\text{tan}}$  has leveled off

with a value of  $\nu_{\text{tan}}$  below  $6 \text{ m s}^{-1}$ . The second criterion searches for the point where the tangential flow becomes less than  $3 \text{ m s}^{-1}$ . Once  $r_f(\theta)$  is determined at each of the 24 azimuthal angles, the extent of the filter domain  $r_0(\theta)$  is then set to  $1.25r_f(\theta)$ : the increase of radius is done in order to make sure that the hurricane component is entirely contained within the filter domain. If  $\nu_{\text{tan}}$  becomes negative anywhere between  $r_f$  and  $1.25r_f(\theta)$ ,  $r_0(\theta)$  is set to the radius of the innermost negative  $\nu_{\text{tan}}$  within the above range.

The determination of the filter domain in the case of Hurricane Florence is illustrated in Fig. 3. The four lines in the figure show radial profiles of  $\nu_{\text{tan}}$  along the northeast, southeast, southwest, and northwest directions, respectively, which are constructed as described above by interpolation of the gridpoint values of the disturbance winds. The black circles on the curves indicate  $r_f(\theta)$  in each respective direction. It is seen that the radii in the southwest and northwest directions are determined by the above-mentioned first criterion, whereas those in the northeast and southeast directions are based on the second criterion. The extent of the filter domain is indicated by the letter symbol  $r_0$  on each profile. Notice the small filter radius in the northeast direction. In general, if a strong nonhurricane disturbance exists in certain directions in the vicinity of the storm, it can cause a discernible feature, such as a large negative and/or positive value, in the profiles of  $\nu_{\text{tan}}(r, \theta)$  in these directions. Then, one of the cutoff criteria in the profile test will be met at a relatively small radius; thereby, the nonhurricane disturbance is retained outside of the filter domain. In the present case, as clearly indicated from the northeast profile, the above situation existed in the northeastern sector where the obtained extent of the filter domain is small (Fig. 2, thick solid lines).

#### d. Construction of the environmental field

As mentioned before, the construction of the environmental field requires the nonhurricane component of the disturbance field. This field is determined for each of the model variables (wind, temperature, surface pressure, and water vapor mixing ratio) at each model level. Through this step of initialization, the analyzed storm, that is, the hurricane component, is in effect removed from the global analysis.

For simplicity, the filter domain is assumed to be independent of height and is applied to all model levels. At the boundary of the filter domain, the disturbance values of any model variable are assumed to be entirely due to the nonhurricane component. Within the filter domain, the disturbance is supposedly dominated by the hurricane component near the center, but the nonhurricane component becomes important near the boundary. Compared to KBR, the present work uses a more objective determination of this component. It is estimated by optimum interpolation (Gandin 1963)

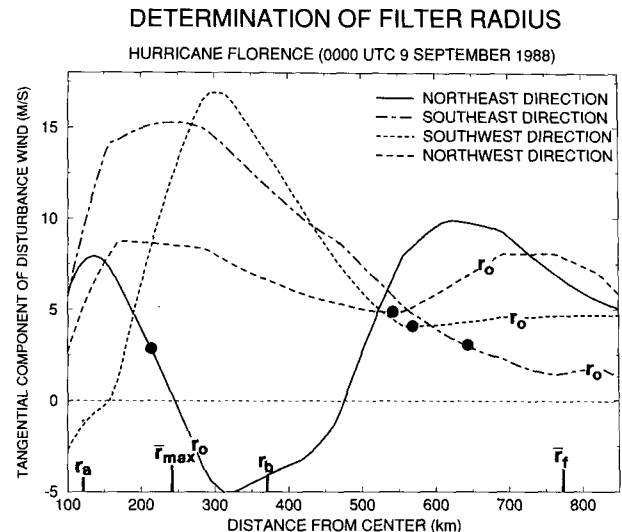


FIG. 3. Profiles of the tangential component of the low-level ( $\sigma = 0.85$ ) disturbance winds in the northeast, southeast, southwest, and northwest directions in case of Hurricane Florence, 0000 UTC 9 September 1988. The radius  $r_f$ , which was determined through the profile test, and the filter radius derived from it are indicated on each profile by a closed circle and the letter  $r_0$ , respectively. The four radii,  $r_a$ ,  $r_b$ ,  $r_{\text{max}}$ , and  $r_f$ , are plotted at the corresponding positions on the abscissa. They are referred to in appendix A and used to determine the starting radius of the profile test.

from the nonhurricane values along the boundary of the filter domain,  $r_0(\theta)$ , and a first-guess value of zero within  $r_0(\theta)$ . This versatile interpolation scheme is well suited to the present approach in which an obtained domain boundary varies from case to case. A brief description of the formulas used is given in appendix B.

The optimum interpolation scheme generates the nonhurricane components that smoothly vary within the filter domain and continuously connect across the domain boundary to the outside nonhurricane field, that is, the disturbance field. Figure 2c shows the nonhurricane component thus determined for the low-level disturbance winds in the case of Hurricane Florence. The difference between the total disturbance (Fig. 2b) and the nonhurricane component (Fig. 2c) identifies the portion of the global analysis that is removed through this phase of the initialization (Fig. 2d).

The nonhurricane component (Fig. 2c) is now combined with the basic field (Fig. 1b) to construct the environmental field. The resulting field (Fig. 4b) is identical to the global analysis (Fig. 4a) except within the filter domain from which the analyzed tropical cyclone is effectively removed. Thus, the splitting of the global analysis into the basic and disturbance fields (section 2b) has no effect on the environmental field outside of the filter domain. Within the filter domain, the environmental field depends on the splitting of the analysis among the basic field and the hurricane and nonhurricane components as described above.

**HURRICANE FLORENCE  
(0000 UTC 9 SEPTEMBER 1988)**

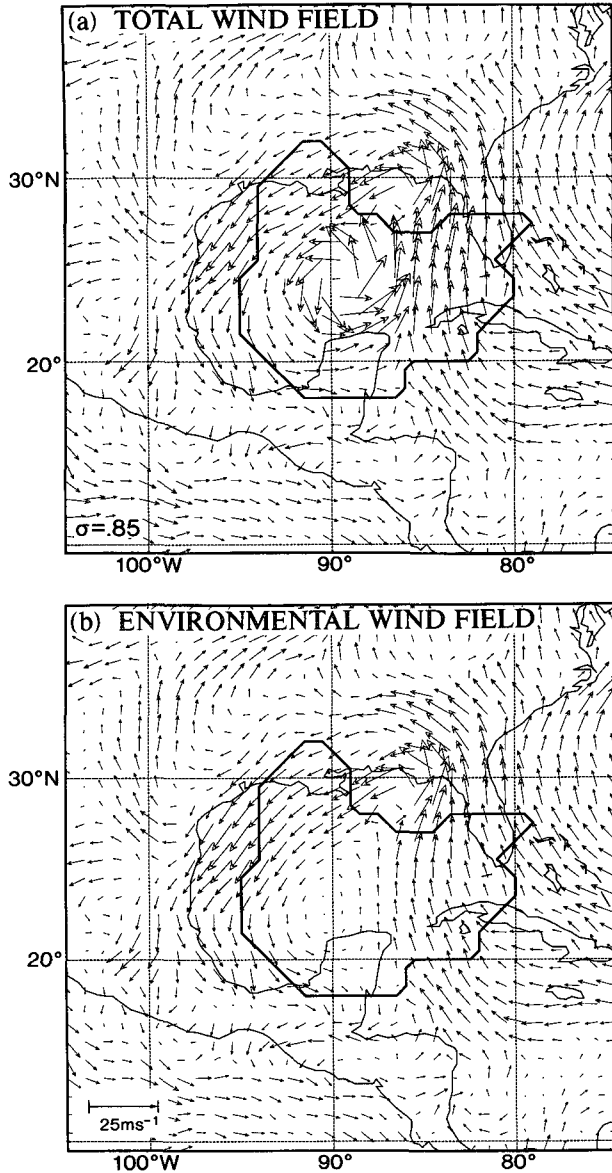


FIG. 4. (a) The original total wind field (same with Fig. 1a) and (b) the environmental wind field obtained using the new initialization method. The filter domain is indicated in each panel by a thick solid line.

*e. Vortex generation*

The scheme to generate a model-compatible vortex is basically the same as the one proposed in KBR. In this scheme, a symmetric vortex is generated from the time integration of the axisymmetric version of the hurricane prediction model starting from a motionless initial condition. During the integration, the tangential component of wind is gradually forced toward the tar-

get profile based on standard storm observations compiled at the National Hurricane Center (NHC). The use of two timescales in the forcing, that is, a long timescale for storm development and a much shorter timescale for relaxation, is an important feature of the present scheme of the vortex generation yielding almost the same wind profile as the target one. Some small changes made to the original version of the computational procedures are described below. These changes serve to produce reasonable initial wind fields in a variety of input data situations.

A minor modification is made in the computation of the target wind profile. In KBR, the storm wind profile was estimated first for each of the four quadrants by adding a correction to the first-guess profile. The correction for each quadrant was computed using the reported winds in the storm advisories and bulletins. Then the four profiles were averaged to yield the target profile. In the new scheme, this process is modified so that a quadrant having unreliable wind data is excluded from the target profile computation. Also, the treatment of the maximum wind data is modified. Usually, the report of the maximum wind includes the speed and only the radius, without the azimuthal angle, of its occurrence. In the present scheme, the observed maximum wind speed is assumed to be located at the azimuthal angle where the tangential component of the environmental wind is the strongest rather than at all angles as in KBR. This yields a target wind profile with a better estimate of the peak wind speed than was obtained by the previous scheme.

The axisymmetric version of the hurricane model is integrated in time to generate the symmetric vortex. In the model equations, the vertical diffusion terms are evaluated by a turbulence closure scheme with a background diffusion coefficient added. It was found that the temperature difference  $\Delta T$  in the initial condition between the sea surface and the lowest model level ( $\sigma = 0.995$ ) at times became as large as several kelvins. In such cases, the convective turbulent mixing that originated near the sea surface might become very strong. Accordingly, if the value of  $\Delta T$  is found to exceed 1 K during the vortex generation, the background diffusion coefficient used for the momentum ( $1 \sigma^2 \text{ m}^2 \text{ s}^{-1}$ ) and that for the temperature and moisture ( $0.5 \sigma^2 \text{ m}^2 \text{ s}^{-1}$ ) are respectively multiplied by the factor  $\Delta T$ . Thus, the generated boundary layer structure is much smoother than that obtained without increasing the background diffusion.

The remaining initialization procedures include the generation of the storm beta gyre through the time integration of a simplified vorticity equation (Ross and Kurihara 1992). The induced gyre is dynamically consistent with the above-obtained symmetric wind, since the latter is used to generate the former. It is noted here that the factor  $1/n$  on the right-hand side of Eq. (2.9) in their paper is an error and has been removed with negligible effect (Wang 1993, personal communica-

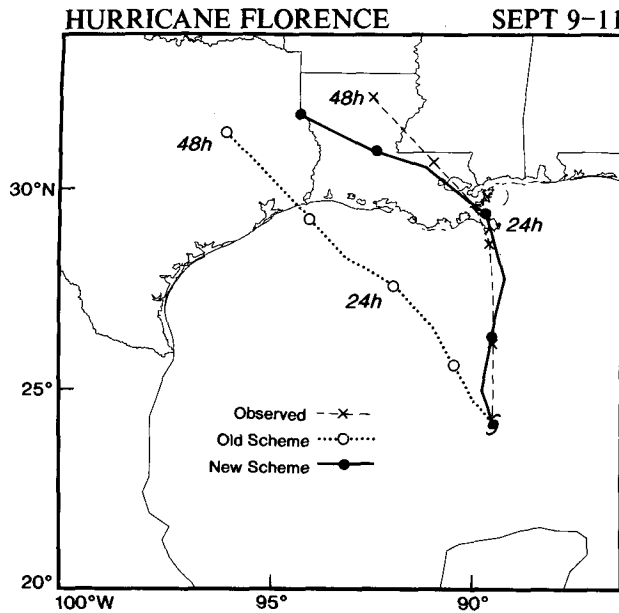


FIG. 5. The track forecasts for Hurricane Florence, 0000 UTC 9 September 1988, starting from the initial conditions determined by the new initialization scheme and by the old scheme (KBR). The observed track is also plotted. The symbols indicate the positions at 12-h intervals.

tion). The generated symmetric vortex (expressed in the form of a deviation from the environmental field) and the asymmetric wind are placed at the observed position and merged with the environmental field. The readjustment of the mass field, the final step in the initialization procedure, is identical to the previous scheme.

#### f. Test of the new scheme

The storm motion is directly affected by the environmental wind. In the case of Hurricane Florence, whether the circulation to the northeast of the storm in the initial condition was retained as in the present scheme or removed along with the analyzed vortex as in the original KBR scheme caused a difference in the environmental flow in the storm region. Figure 5 shows the comparison of the track forecasts using the new and old schemes and indicates considerable reduction of forecast track error with the new scheme. The improvement in the track forecast in this case is apparently due to the improvement in the representation of the initial environmental flow near the storm.

The new scheme is effective if the analyzed vortex is properly removed and the obtained environmental field is accurate. However, these ideal conditions are not necessarily met in all cases because the separation of the analyzed vortex is not unique and the global analysis is not perfect. Certain environmental features that are retained in the storm's surroundings with the

use of the new scheme may not always contribute to the improvement of the track forecast. The new scheme was compared with that of KBR for 23 cases selected from the 1992 and earlier hurricane seasons (Table 1). On the average, the track forecast errors were reduced by the new scheme, especially at early forecast times. About two-thirds of the cases were improved at 12, 24, and 36 h.

### 3. Forecasting with the upgraded prediction system

Implementation of the improved initialization technique before the start of the 1993 hurricane season was part of the upgrading of the GFDL hurricane prediction system. Automated quality checking of the input data and efficient dissemination of the forecast results were also carried out in the new system. The input data to the system are the global analysis and forecast fields imported from NMC, as well as storm information such as the size, intensity, and wind strength obtained from the NHC bulletins. The forecast results from the GFDL system include the storm position and maps showing the storm track and distribution of the low-level maximum winds. The entire prediction system, including data acquisition (about 6 h after the synoptic time), model initialization, time integration of the model, and dissemination of the forecast results to NMC and NHC (12–14 h after the synoptic time), was run in an automated mode without human intervention once the name of the target storm was designated.

During the 1993 hurricane season, the GFDL hurricane prediction system produced 36 forecasts in the Atlantic basin and 36 in the east Pacific basin. In the Atlantic basin, the GFDL system performed exceptionally well for cases of Hurricane Emily. The composite of 72-h forecasts made every 12 h after 1200 UTC 26 August, together with the NHC best-track positions at 6-h intervals, is shown in Fig. 6. The system successfully forecasted the movement of Emily toward the coast of North Carolina and the subsequent abrupt recurvature of the storm just east of Cape Hatteras several days beforehand. The model correctly predicted, over 48 h in advance, the occurrence of winds exceeding hurricane force along the tip of Cape Hatteras. In Table 2, the average forecast position error (relative to the best-track positions) for 14 of the Emily cases predicted by the GFDL model is compared with the error

TABLE 1. Comparison between the new and the KBR scheme.

Forecast period (h)	12	24	36	48
Number of cases	23	23	22	20
Mean position error (km)				
New scheme	85	158	244	311
KBR scheme	96	184	263	321
Percent of cases with the position error reduced by the new scheme	70	65	64	55

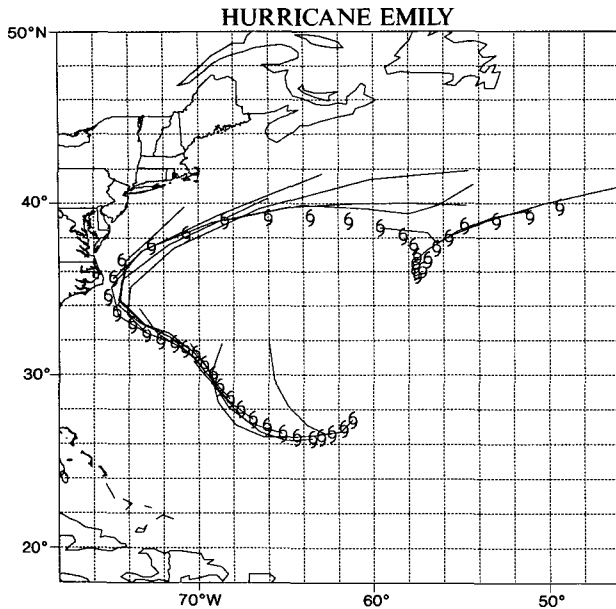


FIG. 6. Composite of the 72-h track forecasts of Hurricane Emily made every 12 h after 1200 UTC 26 August 1993. The hurricane symbols indicate the best-track positions at 6-h intervals.

in the official forecasts (issued before all model forecasts become available) for the same cases and the forecast errors by various other models. Relative to the CLIPER (climatology and persistence) model, forecast improvements by the GFDL system for all 14 cases (difference between the average GFDL error and the average CLIPER error divided by the average CLIPER error) were  $-67\%$ ,  $-72\%$ ,  $-72\%$ , and  $-55\%$  (minus sign indicating improvement) at 24, 36, 48, and 72 h, respectively.

The track prediction of some of the other storms in the Atlantic during the 1993 season revealed problems related to high topography and storm intensity. For example, the forecast of Bret suffered from a consistent northward bias as the weak system moved along the South American coast. The previous algorithm of storm tracking used pressure reduction to sea level. In some cases, this scheme produced a pressure field in which the weak disturbance could not be clearly distinguished from high topographic features. In post-season tests, this difficulty has been significantly alleviated by tracking the pressure disturbance at a height surface near the maximum height of the underlying topography within the fine-mesh area of the MMM model. Also, the model integration is terminated when the storm becomes too weak to be tracked. The storm intensity in the model tended to deviate from the observed value during the early forecast period. It is speculated that the incorrect track forecast of westward-moving Tropical Storm Dennis may have resulted from the erroneous deepening of the weak storm, thereby subjecting it to the southerly flow aloft. In spite of these problems, the

overall forecast improvement relative to the CLIPER forecasts for all 36 Atlantic cases was still favorable for the GFDL prediction system, that is,  $-26\%$ ,  $-32\%$ ,  $-44\%$ , and  $-40\%$  at 24-, 36-, 48-, and 72-h predictions, respectively.

In the eastern Pacific basin, the reductions of forecasted position error by the GFDL system at 24, 36, 48, and 72 h were  $-15\%$ ,  $-27\%$ ,  $-30\%$ , and  $-15\%$  compared with the CLIPER forecasts. At 12 h, the GFDL model position error revealed a directional bias indicating too rapid westward storm movement. Interestingly, other dynamical models showed a similar bias. The cases in which the GFDL model provided good track forecasts include westward-moving systems such as Dora and Eugene, as well as those paralleling the Mexican coast such as Hilary and Lidia. The composite of forecasts of Lidia and the actual positions at 6-h intervals are shown in Fig. 7. In these cases, the GFDL system yielded 20% error reduction from the CLIPER forecast at 12 h and 50% at and beyond 36 h. The GFDL model was the first forecast model that predicted the recurvature of Lidia toward the Pacific coast of Mexico.

#### 4. Summary and remarks

The GFDL hurricane prediction system was upgraded for use in the 1993 hurricane season. In the revised system, the model initialization scheme was improved so that important nonhurricane features in the global analysis were preserved in the initial condition.

The present approach for model initialization is unique in several respects. First, the filter domain containing the analyzed hurricane disturbance is not necessarily circular. By minimizing the region of the analysis that is modified, important features near the storm area can be preserved in the model initial fields. Sec-

TABLE 2. Average forecast position errors (km) for Hurricane Emily by various models: the GFDL system, Official forecast (issued before all model forecasts become available), CLIPER (climatology and persistence) model, two models used at NHC, the model at the AOML/Hurricane Research Division (HRD), and the global (AVN) and hurricane (QLM) models at NMC (run for fewer cases than the GFDL hurricane model).

Forecast period (h)	12	24	36	48	72
Number of cases	14	14	14	14	12
GFDL system	56	78	109	142	304
Official forecast	73	149	225	298	419
CLIPER	87	211	364	513	653
NHC90 (NHC)	80	167	261	341	438
BAM-MEDIUM (NHC)	72	132	186	228	297
VICBAR (HRD)	70	139	224	319	406
AVN (NMC)	91	144	215	335	427
(number of cases)	(13)	(13)	(13)	(12)	(6)
QLM (NMC)	102	166	222	273	358
(number of cases)	(10)	(10)	(10)	(10)	(8)

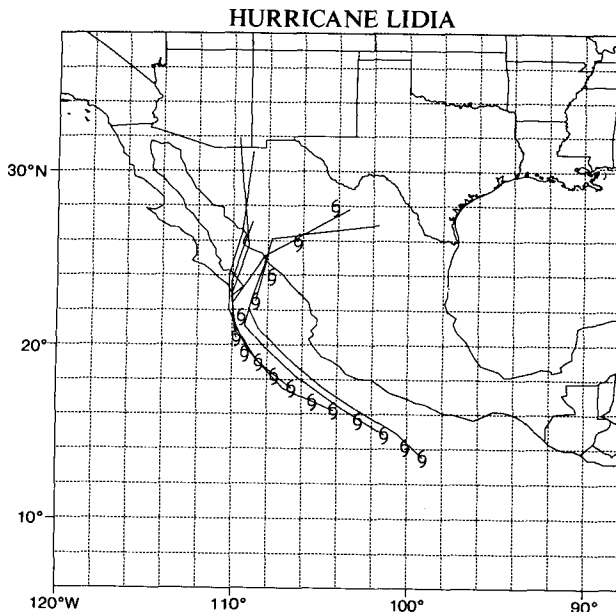


FIG. 7. Composite of the 72-h track forecasts of Hurricane Lidia made every 12 h after 0000 UTC 10 September 1993. The hurricane symbols indicate the best-track positions at 6-h intervals.

ond, an optimum interpolation technique is used to determine the environmental fields within the filter domain. These fields smoothly connect to the fields outside of the domain. Third, the use of the axisymmetric version of the prediction model in the generation of the symmetric component of the new vortex ensures the dynamical consistency in the vortex structure as well as the compatibility of the generated vortex with the physics and resolution of the prediction model. Also, the use of the generated symmetric wind to induce the asymmetric flow makes the latter dynamically consistent with the former. The above type of initialization scheme will remain useful in practice until advanced tropical cyclone analysis techniques such as finescale analysis of the internal structure of storms, application of an adjoint model, or a high-resolution four-dimensional data assimilation method become operationally practical. Furthermore, the present approach is applicable to various other problems involving tropical cyclones such as diagnostic analyses of tropical disturbances, simulation experiments examining sensitivity of tropical storms, or ensemble forecasts of hurricanes.

The improved version of the hurricane prediction system was run in an automated semioperational mode at GFDL for both Atlantic and eastern Pacific storms throughout the 1993 hurricane season. Forecasts of storm motion were satisfactory in many cases, including the sharp recurvature of Hurricane Emily in the Atlantic and the landfall of Hurricane Lidia in the eastern Pacific. The improvement in the track forecasts suggests that the modified initialization scheme produced a better initial condition for the MMM model.

The effectiveness of the new initialization scheme relies on the quality of the input data, that is, the global analysis performed at NMC. If additional observations become available in the region of the storm and its surroundings, they will be valuable for increasing the accuracy of the global analysis. Increased observations will be useful also in the specification of the realistic vortex and can lead to further improvement of the track forecast.

The accuracy of track prediction is also influenced by the forecast of the storm intensity and structure. This implies the need for improvement of the model resolution, in particular in the storm's interior region, through which not only the initial structure of the storm but also the evolution of that structure can be accurately described. The relationship between the motion and structure of the storm should be extensively investigated with the use of such a very high resolution model.

*Acknowledgments.* The authors would like to express their deep appreciation to Jerry Mahlman for his constant encouragement during the pursuit of the present study and to Isidoro Orlanski and Chun-Chieh Wu for their critical reading and valuable comments on the original manuscript. They thank Stephen Lord for his support of their work, for supplying them with the NMC analyses and storm data used in the development of the new scheme, and for a critical review of their paper. They are also grateful to Russell L. Elsberry for constructive comments on the paper. They thank Jeffrey Varanyak and Catherine Raphael for their work in the preparation of the figures.

#### APPENDIX A

##### Starting Radius in the Wind Profile Test for the Filter Domain Determination

The extent of the filter domain in the direction  $\theta$  is determined through the search for the radius  $r_f(\theta)$  defined in section 2c on the radial profile of the tangential component of the disturbance wind  $v_{\tan}(r, \theta)$ . The search begins at a starting radius and proceeds outward until the prescribed criterion mentioned in the text is met. The starting radius should be small enough so that the profile test can proceed over a portion where the profile is predominantly due to the hurricane component but not so small as to include the central region of the storm where the profile is strongly dependent on the position defining the vortex center. In the automated hurricane prediction system, the starting radius is located using a specific interval whose endpoints are determined from the profile of the azimuthally averaged tangential wind  $\bar{v}_{\tan}(r)$ . Specifically, the endpoints are related to the quantity  $\bar{r}_{\max}$  (radius of the maximum  $\bar{v}_{\tan}$ ) and  $\bar{r}_f$  [radius determined through test of the profile  $\bar{v}_{\tan}(r)$ , beginning at the radius  $1.5\bar{r}_{\max}$  and using the same criteria as those used to define  $r_f$ ] by the following formulas:

$$r_a = a\bar{r}_{\max}, \quad r_b = b\bar{r}_{\max} + (1 - b)\bar{r}_f.$$

Presently, the parameters  $a$  and  $b$  are set to the empirically chosen appropriate values 0.5 and 0.75, respectively. The inner endpoint  $r_a$  and the outer endpoint  $r_b$  thus computed as well as  $\bar{r}_{\max}$  and  $\bar{r}_f$  in the case of Hurricane Florence are indicated in Fig. 3. Given the range  $[r_a, r_b]$ , the starting radius for the direction  $\theta$  is determined as follows. Let the radius of the maximum  $\nu_{\tan}$  along this direction within the 1200-km distance be  $r_m(\theta)$ . If  $r_m(\theta)$  is not in the range  $[r_a, r_b]$ , then  $r_m(\theta)$  is reset to the radius of the outermost relative maximum  $\nu_{\tan}$  within the range  $[r_a, r_b]$  if such a relative maximum exists and  $\nu_{\tan}$  is cyclonic between that radius and  $r_b$ . If such a maximum does not exist within  $[r_a, r_b]$ , then  $r_m(\theta) = r_b$ . Finally, the starting radius is set to  $1.1r_m(\theta)$ . Thus, the starting radius is bounded by  $1.1r_a$  and  $1.1r_b$ .

APPENDIX B

Application of the Optimum Interpolation Method

In the present study, the idea of optimum interpolation (Gandin 1963) is applied to construct fields of the nonhurricane component within the filter domain. Interpolation formulas used in the present scheme are described below.

In the general framework of an univariate optimum interpolation, a guess field is given for a quantity  $h$ , while observed or prescribed values of  $h$  are known at a finite number of points  $i$  ( $i = 1, \dots, N$ ). Let  $h_p^g$  be the guess value at the point  $p$ , and  $h_i^g$  and  $h_i^0$  be, respectively, the guess value and the known (input) value at the point  $i$ . The estimate of  $h$  at a point  $p$ ,  $h_p^e$ , is made by making a correction to the guess value at the point  $p$  as follows:

$$h_p^e = h_p^g + \sum_{i=1}^N w_{pi}(h_i^0 - h_i^g), \quad (\text{B.1})$$

where  $w_{pi}$  denotes the weight of contribution from the point  $i$  to the point  $p$ . Denoting the error of  $h_i^g$  and  $h_i^0$  by  $\delta h_i^g$  and  $\delta h_i^0$ , respectively, the error of  $h_p^e$ , denoted by  $E_p$ , is given as

$$E_p = \delta h_p^g + \sum_{i=1}^N w_{pi}(\delta h_i^0 - \delta h_i^g). \quad (\text{B.2})$$

In the present case, the guess field (of the nonhurricane component of the disturbance field) is set to zero everywhere in the filter domain because the disturbance in this region is supposedly dominated by the hurricane component. The input data  $h_i^0$  are the disturbance field values at points at the filter radii [denoted by  $r_0(\theta)$  in the text] in 24 directions. (They are obtained from the disturbance values at the surrounding grid points by

bilinear interpolation.) By setting  $\delta h_i^0 = 0$  in order that the field of  $h$  smoothly changes across the boundary of the filter domain, (B.1) and (B.2) become, respectively,

$$h_p^e = \sum_{i=1}^{24} w_{pi}h_i^0 \quad (\text{B.3})$$

and

$$E_p = \delta h_p^g - \sum_{i=1}^{24} w_{pi}\delta h_i^g. \quad (\text{B.4})$$

Provided that the statistics of the guess-value error is known, a set of weights  $w_{pi}$  for the point  $p$  can be determined from the condition that the statistical or ensemble mean of the estimation error square at the point  $p$  is minimized; that is,

$$\frac{\partial \overline{(E_p)^2}}{\partial w_{pi}} = 0 \quad i = 1, \dots, 24. \quad (\text{B.5})$$

The above requirement yields 24 linear equations,

$$\sum_{j=1}^{24} w_{pj}\mu_{ij} = \mu_{pi} \quad i = 1, \dots, 24, \quad (\text{B.6})$$

where  $\mu_{ij}$  denotes the correlation coefficient of the guess-value error between the two points  $i$  and  $j$ . The value of  $\mu_{ij}$  depends on the separation distance  $d$  between the two points. In a conventional form it is expressed by  $\exp[-(d/D)^2]$ , where  $D$  is the distance scale of the correlation decrease (250 km in the present study). To perform the optimum interpolation to a grid point within the domain, first 24 linear equations (B.6) are solved for weights, and then the optimum value is computed by (B.3) combining the 24 disturbance values on the filter boundary with a set of 24 weights obtained. It is noted here that in solving (B.6), a nonnegative least squares solution is used rather than an accurate solution that may be numerically ill behaved.

REFERENCES

Anthes, R. A., 1982: *Tropical Cyclones, Their Evolution, Structure, and Effects*. Amer. Meteor. Soc., 208 pp.

Bender, M. A., R. J. Ross, R. E. Tuleya, and Y. Kurihara, 1993: Improvements in tropical cyclone track and intensity forecasts using the GFDL initialization system. *Mon. Wea. Rev.*, **121**, 2046–2061.

Gandin, L. S., 1963: *Objective Analysis of Meteorological Fields*. Gidrometeorologicheskoe Izdatel'stvo, (Leningrad; Israel Program for Scientific Translations) Jerusalem, 242 pp.

Kurihara, Y., M. A. Bender, and R. J. Ross, 1993a: An initialization scheme of hurricane models by vortex specification. *Mon. Wea. Rev.*, **121**, 2030–2045.

—, R. E. Tuleya, M. A. Bender, and R. J. Ross, 1993b: Advanced modeling of tropical cyclones. *Tropical Cyclone Disasters*, J. Lighthill, Z. Zhemina, G. Holland, and K. Emanuel, Eds., Peking University Press, 190–201.